

# Diffusion of lithium in electrodeposited vanadium oxides

Ed Andrukaitis<sup>a,\*</sup>, Ian Hill<sup>b</sup>

<sup>a</sup> Defence R&D Canada Atlantic (Attn:H/AVRS), National Defence Headquarters, 101 Colonel by Drive, Ottawa, Ont., Canada K1A 0K2

<sup>b</sup> Institute for Chemical Process and Environmental Technology, National Research Council of Canada, Ottawa, Ont., Canada K1A 0R6

Available online 1 June 2004

## Abstract

Using a novel electrodeposition/thermal process,  $V_6O_{13+y}$ ,  $0 < y < 2$ , bronzes were directly fabricated into a coin cell without the use of binders or electronic conductors. Transport properties of lithium insertion and removal from  $V_2O_5$  and nonstoichiometric (ns)  $V_6O_{13+y}$  bronzes, were examined by electrochemical methods in asymmetrical  $Li/Li_xV_6O_{13+y}$  cells. Diffusion coefficients in the range  $0.2\text{--}5.0 \times 10^{-8} \text{ cm}^2 \text{ s}^{-1}$  were found for insertion and removal steps in the range,  $x = 0\text{--}1.0$ . The transport of lithium ions from the vanadium oxides is similar to the insertion process. These bronze cathodes have similar transport properties to composite cathodes, making them potentially useful for electrochromic displays and microbatteries.

© 2004 Elsevier B.V. All rights reserved.

**Keywords:** Lithium removal; Lithium intercalation; Vanadium oxide; Transition metal oxides; Vanadium oxide bronzes; Lithium ion diffusion

## 1. Introduction

The introduction and use of lithium ion batteries in the commercial world is widespread; however, their use in military portable electronics has progressed at a much slower pace for several reasons. First, using a rechargeable battery where a primary “disposable” battery was used adds to maintenance costs (charging facilities), even though there are savings from the amount of batteries procured. Secondly, rechargeable batteries typically have lower energy densities and much poorer low temperature performance compared to primary lithium batteries. Although strides are being made in these latter areas, the charging of lithium batteries is another important factor in military operations because, for many applications, “fast” charge capability is needed. Fast removal of ions is also needed for electrochromic devices. Vanadium oxides have been studied both for application in lithium batteries, because of their potentially high specific capacity, and for devices that take advantage of their electrochromic properties.

A great deal of effort has gone towards trying to interpret the kinetic mechanism of the insertion of ions into several chalcogenides; however, most of the emphasis has been on examining the insertion properties, with limited work on the ion removal mechanism from a solid electrode. Most of the

redox studies have been made on thin films of various transition metal oxides for electrochromic materials. A model, based on the space-charge limited diffusion mechanism has been described for the bleaching (oxidation) of  $WO_3$  electrochromic films by Faughnan et al. [1,2], where the current decays as  $t^{-3/4}$  over long times for these amorphous thin  $WO_3$  films.

In the present study, crystalline  $V_2O_5$  and non-stoichiometric (ns)  $V_6O_{13+y}$  bronzes were electrodeposited onto a conducting substrate, with no binders or electronic conducting materials needed to fabricate the cathode for a coin cell. These asymmetrical cells, with a pure crystalline vanadium oxide cathode, were thought to be very useful in studying Li intercalation and removal properties without any interference from traditional electrode additives in the solid state electrode (SSE). Initial results of the transport properties, plus possible mechanisms of insertion and removal of lithium from these bronzes, are discussed in this paper.

## 2. Experimental

Electrodeposition of hexavanadates onto a conducting substrate, plus heating to form vanadium oxide bronze electrodes, have been described in detail elsewhere [3]. Solutions for electrodeposition of  $NH_4VO_3$  solution were prepared at  $50^\circ\text{C}$  [4]. Electrodeposits were formed on conducting substrates of 150 stainless steel mesh and

\* Corresponding author. Tel.: +1-613-990-0638; fax: +1-613-993-4095.  
E-mail address: [ed.andrukaitis@nrc-cnrc.gc.ca](mailto:ed.andrukaitis@nrc-cnrc.gc.ca) (E. Andrukaitis).

decomposed at temperatures from 300 to 350 °C under air or argon atmospheres. Cathodes of the bronzes were prepared in a coin cell using an electrolyte composed of 1M LiPF<sub>6</sub> dissolved in 1:1 of ethylene carbonate and dimethyl carbonate (EC:DMC). The counter electrode was Li metal [3]. Cells were discharged and then charged galvanostatically, potentiostatically or a linear sweep voltammetry (CV), using a PAR Model 273 Potentiostat with electrochemical software.

### 3. Theory

Two electrochemical methods, chronoamperometry and chronopotentiometry, have been applied to asymmetrical Li/Li<sub>x</sub>V<sub>2</sub>O<sub>5</sub> and nonstoichiometric (ns) V<sub>6</sub>O<sub>13</sub> coin cells. The average chemical diffusion coefficient of Li<sup>+</sup> ions in Li/Li<sub>x</sub> vanadium oxide can be determine by the total depletion of Li<sup>+</sup> ions in the SSE at the electrolyte/Li<sub>x</sub>SSE interface, by passing a high galvanostatic current through the Li/Li<sub>x</sub>SSE cell. The method was discussed by Honders et al. [5] for a three electrode system but, although electrolyte breakdown is inevitable for cell voltages above approximately 4 V, the ability to use this technique for asymmetrical coin cells was attempted in the present investigation. When the total depletion of Li ions occurs, another electrode process usually starts, which can be observed in the overvoltage–time behaviour of the cell. The relationship between depletion time (*t<sub>d</sub>*) and the average chemical diffusion coefficient (*D<sub>AV,Li<sup>+</sup></sub>*) is given by:

$$(D_{AV,Li^+})^{0.5} = \frac{2I}{AFc^*} \left( \frac{t_d}{\pi} \right)^{0.5} \quad (1)$$

If *t<sub>d</sub><sup>0.5</sup>* is proportional to *I<sup>-1</sup>*, the “breakdown-time” corresponds with the total depletion of the Li<sup>+</sup> ions in the SSE.

The formulae in Honders et al. [5] can also be used for a potentiostatic voltage step applied to an asymmetrical Li/Li<sub>x</sub>V<sub>2</sub>O<sub>5</sub> cell. The method involves the application of a small ( $\Delta E \ll RT/F$ ) potentiostatic voltage step to an asymmetrical cell. The response function for the current, if total cell resistance *R<sub>tot</sub>* may be neglected, is given by:

$$I(\tau) = -\frac{2\Delta E}{Z_o} \sum \exp \left[ -\frac{(2n+1)2\pi^2\tau}{4} \right] \quad (2)$$

*R<sub>tot</sub>* = *R<sub>Ω</sub>* + *R<sub>ct</sub>*, where *R<sub>Ω</sub>* is the ohmic resistance of the electrolyte and the electrodes and *R<sub>ct</sub>* is a charge transfer resistance of one or two of the interfaces.

The normalized current (*I<sub>n</sub>*) is defined by:

$$I_n = \frac{I(\tau)Z_o\pi^{0.5}}{\Delta E} \quad (3)$$

In the above equations, *D* is the chemical diffusion coefficient of the Li<sup>+</sup> in V<sub>2</sub>O<sub>5</sub> or V<sub>6</sub>O<sub>13</sub>, *c\** the equilibrium concentration of Li<sup>+</sup> ions in the SSE, *I* the current, *A* the active electrode area, *δ* the (longitudinal) length of the diffusion

path of the Li<sup>+</sup> ions, *Z<sub>o</sub>* the interface resistance, *τ* the characteristic relative time and *t* the time [5].

For this ideal behaviour, the tangent of the log *I<sub>n</sub>* versus log *τ* curve for *τ* < 0.25 equals −0.5.

If *R<sub>tot</sub>* cannot be neglected, when *τ* < 0.25, the current response is given by:

$$I(\tau) = \frac{\Delta E}{R_{tot} + Z_o/3} \exp \left[ \frac{Z_o\tau^{0.5}}{R_{tot}} \right]^2 \operatorname{erfc} \left[ \frac{Z_o\tau^{0.5}}{R_{tot}} \right] \quad (4)$$

And for *τ* > 0.25 by:

$$I(\tau) = \frac{\Delta E}{R_{tot} + Z_o/3} \exp \left[ -\frac{\tau/R_{tot}}{Z_o + 1/3} \right]. \quad (5)$$

A nearly linear curve occurs when *I<sup>-1</sup>* versus *t<sup>0.5</sup>* is plotted. The value of *R<sub>tot</sub>* can be obtained by extrapolating the *I<sup>-1</sup>* versus *t<sup>0.5</sup>* curve to *t* = 0. For long times, Honders and Broers [6] determined that the following equation could be derived from (5) for *I<sub>n</sub>* in logarithmic form as:

$$\log(I) = \log \left( \frac{\Delta E}{R_{tot} + Z_o/3} \right) - \frac{Dt}{2.303\delta^2} \left( \frac{R_{tot}}{Z_o + 1/3} \right) \quad (6)$$

where

$$\tau = \frac{Dt}{\delta^2} \quad (7)$$

The plot of log *I* versus *t* from Eq. (6) for *τ* > 0.25 yields a straight line; extrapolation back to *t* = 0, yields *R<sub>tot</sub>* + *Z<sub>o</sub>*/3. Since *R<sub>tot</sub>* has been calculated above, then *Z<sub>o</sub>* is also know and a value for *D* can be determined from the slope of the linear part in (6). By extrapolation of the intercept of log *I* versus *t* axis for *t* = 0 and from the slope of this curve from (6), the value of thermodynamic coefficient, *K<sub>t</sub>*, can be found from the equation [6]:

$$Z_o = \frac{K_t RT \delta}{F^2 c^* D (\Omega \text{ cm}^2)} \quad (8)$$

From Eqs. (6) and (7), an approximate value for *D* can be obtained by substituting the value of *R<sub>tot</sub>* and filling in for *τ* and *Z<sub>o</sub>*.

Measurement of the Li<sup>+</sup> diffusion coefficient could also be obtained using the potentiostatic intermittent titration technique (PITT) [7]. In this method the plateau in the *It<sup>1/2</sup>* versus log *t* graph represents the Cottrell region and this was used to calculate the diffusion coefficient for Li<sup>+</sup> from the equation:

$$It^{1/2} = \frac{D^{1/2} \Delta Q}{l\pi^{1/2}} \quad (9)$$

where  $\Delta Q$  is the amount of charge inserted or removed during the potential step and *l* the film thickness.

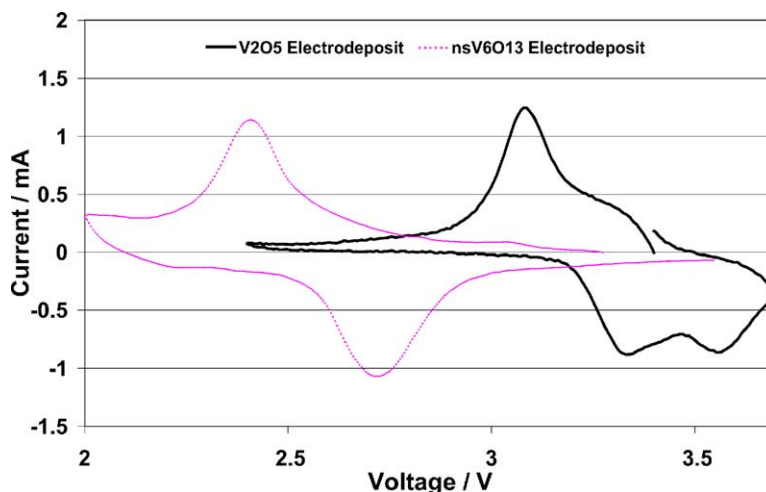


Fig. 1. Cyclic voltammetry plot of the  $\text{Li}_x\text{V}_2\text{O}_5$  and  $\text{nsLi}_x\text{V}_6\text{O}_{13+y}$  cathode electrodes in a coin cell with a Li metal anode and 1M  $\text{LiPF}_6$  in 1:1 EC:DMC electrolyte at a scan rate of  $50 \mu\text{V s}^{-1}$ .

## 4. Results

### 4.1. Physical characteristics of the bronzes

Using the electrodeposition method to form hexavanadates, followed by a thermal decomposition from 300 to  $350^\circ\text{C}$ ,  $\text{V}_2\text{O}_5$  was formed in air and nonstoichiometric  $\text{V}_6\text{O}_{13}$  was formed in Argon the process has been discussed in detail elsewhere [8]. The  $\text{V}_6\text{O}_{13}$  is slightly oxygen rich with the stoichiometry of  $\text{V}_6\text{O}_{13.2}$ . It has been found that this stoichiometry has better electrochemical characteristics [9,10]. These vanadium oxide bronzes are directly fabricated into a coin cell design without the need for binders or electronic conductors. Good contact between the active material and the substrate, plus consistent physical properties, can provide electrodes for studying the transport and kinetic properties for lithium insertion and removal.

The lithium intercalation and removal of an asymmetrical  $\text{Li}/\text{Li}_x\text{V}_2\text{O}_5$  and  $\text{nsV}_6\text{O}_{13}$  cell by cyclic voltammetry is shown in Fig. 1. The  $\text{V}_2\text{O}_5$  or  $\text{nsV}_6\text{O}_{13}$  bronzes show very good cycling behaviour with hundreds of cycles possible [9]. This demonstrated that durability and adherence to the substrate is very good in the coin cell design and that the utilisation of the active material is also good. Estimates of the thickness and area, for the calculation of transport properties, was complicated by surface roughness and the shape of the bronzes on the stainless steel mesh substrate, as shown in Fig. 2. However, the surface was uniformly similar in crystal size, thickness and geometry for all cathodes fabricated into coin cells for electrochemical studies. Thus, once an average thickness and surface area was estimated, it was possible to apply them as constants in the calculations over a number of cells, because several cathode electrodes are produced in a large batch yielding very similar mass and morphology in either bronze stoichiometry for the electrochemical studies.

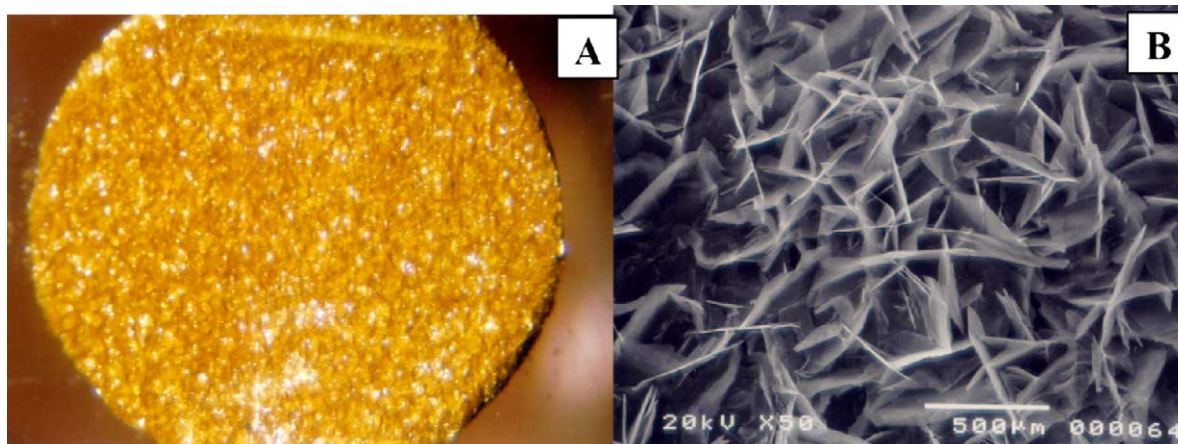


Fig. 2. Photograph of a vanadium pentoxide bronze electrodeposit after heating to  $350^\circ\text{C}$  on a stainless steel mesh substrate. (A) Magnification of  $6.5\times$  with microscope and (B) magnification at  $50\times$  by scanning electron microscopy.

#### 4.2. Transport properties of lithium insertion and removal

The determination of the chemical diffusion coefficients of  $\text{Li}^+$  ions in  $\text{Li}/\text{Li}_x\text{V}_2\text{O}_5$  and  $\text{nsV}_6\text{O}_{13}$  by different electrochemical methods, as well as the thermodynamic factor  $K_t$  (kinetic) are summarised below. Representative plots of the chronoamperometric experiments are shown in Fig. 3A–C.

From the plateau in the  $I t^{1/2}$  versus  $\log t$  plot, which represents the Cottrell region in Fig. 3A, the lithium ion chemical

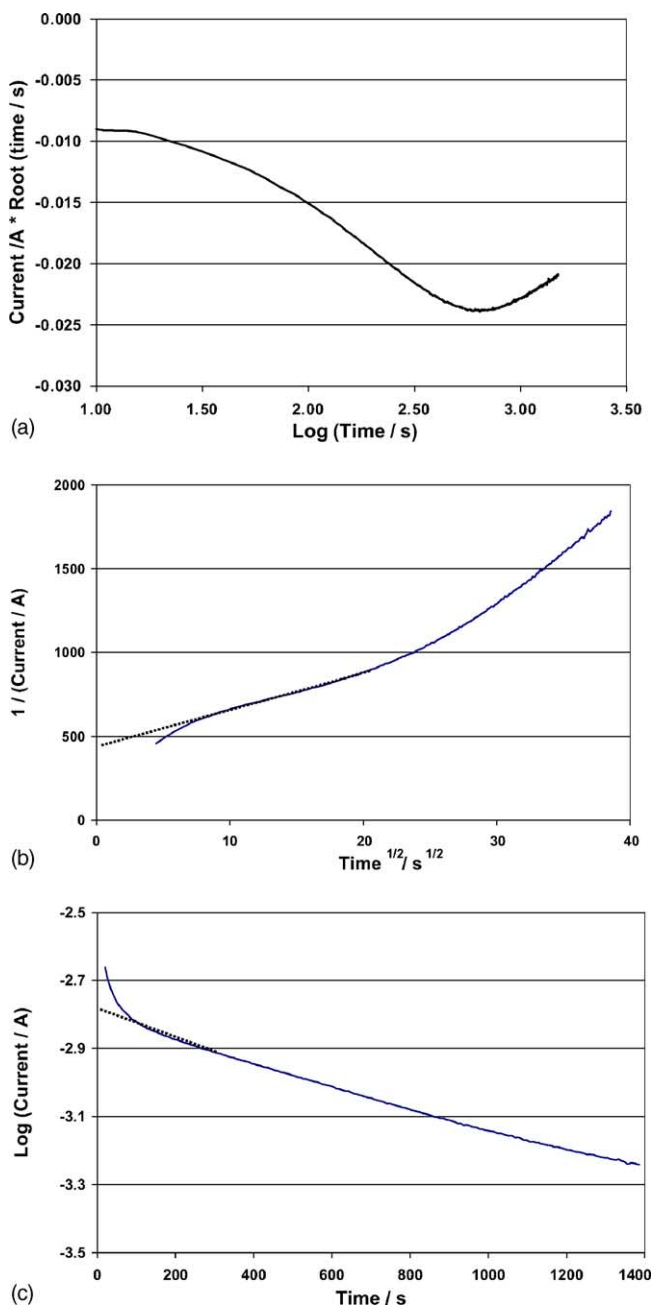


Fig. 3. Plot of the current response resulting from the application of a voltage step of 50 mV to the  $\text{Li}/\text{Li}_x\text{V}_6\text{O}_{13+y}$  coin cell with 1M  $\text{LiPF}_6$  in 1:1 EC:DMC electrolyte.  $x = 0.89\text{--}0.84$  ( $c_{\text{Li}^+}^* = 1 \times 10^4 \text{ mol m}^{-3}$ ),  $A = 1.267 \times 10^{-4} \text{ m}^2$ ,  $\delta = 2.5 \times 10^{-4} \text{ m}$ ,  $T = 23^\circ \text{C}$ ,  $l = 5.0 \times 10^{-5} \text{ m}$ .

diffusion coefficient ( $D$ ) was calculated from Eq. (9). Also, by application of the long-time potentiostatic step method used by Honders et al. [5], it is clear that a total resistance ( $R_{\text{tot}}$ ) is present as shown in Fig. 3B, otherwise the ideal behaviour in Eq. (2) would apply and the  $I^{-1}$  versus  $t^{0.5}$  curve would extrapolate to zero for  $t = 0$ . A value of about  $500 \Omega$  was obtained for  $R_{\text{tot}}$  using Eq. (4) in this example. A value for the thermodynamic coefficient  $K_t$  (kin) of 59 was found from the slope and intercept of the  $\log I$  versus  $t$  plot in Fig. 3C using Eq. (8) and solving for  $Z_0$  in Eq. (6). By applying Eq. (6) a value for  $D$  can be obtained by substituting the value of  $R_{\text{tot}}$  and filling in for  $\tau$  and  $Z_0$ . A value of  $3.8 \times 10^{-9} \text{ cm}^2 \text{ s}^{-1}$  was obtained from the same data. This is in good agreement with the value for  $D$  obtained by the PITT method shown in Fig. 3A where a value of  $1.1 \times 10^{-8} \text{ cm}^2 \text{ s}^{-1}$  was calculated. However, it was thought that the first number, obtained by the long-time potentiostatic step method, had a much larger margin of error by this method because the value of  $R_{\text{tot}}$  is only an approximation.

Using a high current pulse method, the chemical diffusion coefficient was also calculated using Eq. (1). It was experimentally verified that  $t_d^{0.5} \propto I^{-1}$ . This indicates that the “breakdown-time” indeed corresponds with total depletion of the Li ions in the solid electrode at the electrolyte/ $\text{Li}/\text{Li}_x\text{V}_2\text{O}_{5-y}$  interface.

The depletion time was calculated as shown in Fig. 4 by the knee that occurs in the voltage versus time plot.

It is at this point that the Li ions are totally depleted at the electrolyte/solid cathode interface and, typically, another electrode process starts. Using this technique at a similar value of  $x$  for  $\text{Li}_x\text{V}_6\text{O}_{13}$  above, for lithium ion removal, a value of  $1.9 \times 10^{-8} \text{ cm}^2 \text{ s}^{-1}$  was calculated. The method proved not to be destructive over the short-term because, after interruption of the current pulse the potential returned to its initial value. It appears that only a very thin layer of the cathode material at the electrolyte/SSE interface is involved in the depletion process. While the PITT and long term chronopotentiometry methods are more time consuming, the use of the depletion method only involves a short time. This

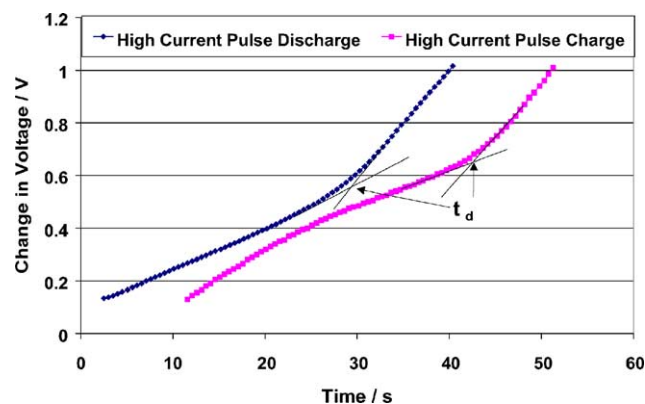


Fig. 4. Plot of change in voltage against time for the high current pulse method to a  $\text{Li}/\text{Li}_x\text{V}_6\text{O}_{13.2}$  ( $x = 0.81$ ) asymmetrical lithium coin cell. Current pulse charge of 20 mA was applied for approximately 50 s.

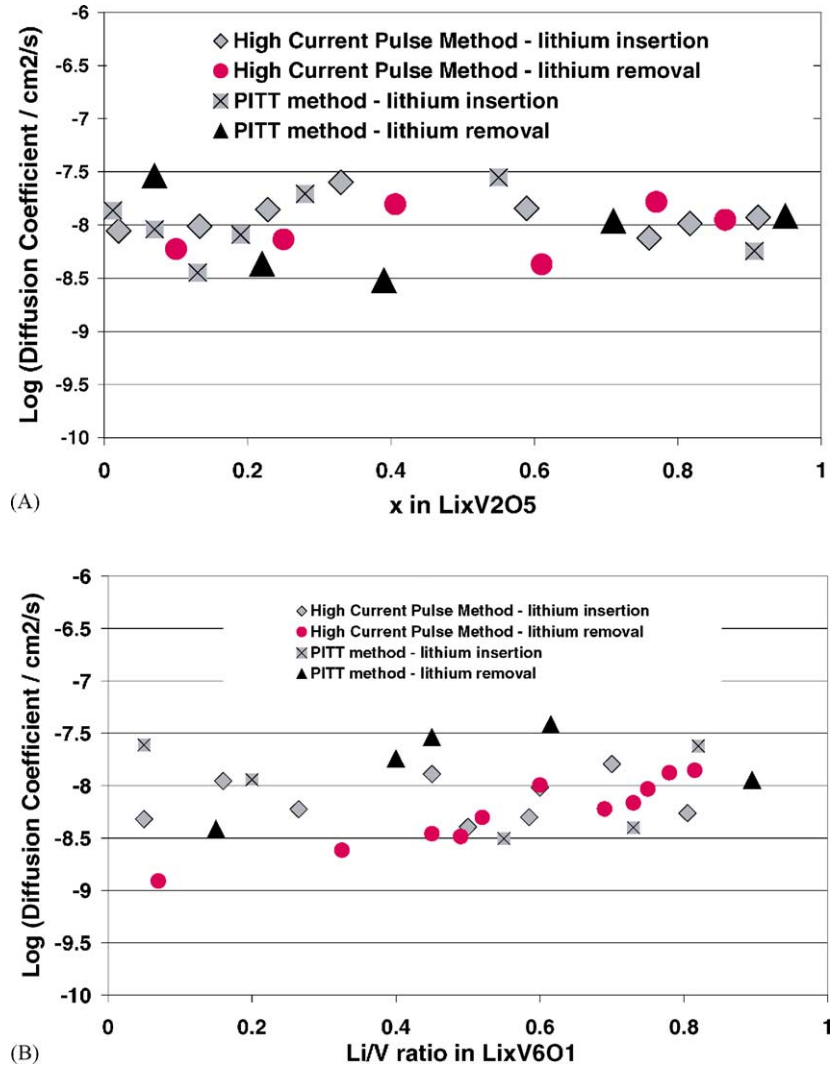


Fig. 5. Plot of lithium ion chemical diffusion coefficients for cathodes of  $\text{Li}/\text{Li}_x\text{V}_2\text{O}_5$  and  $\text{nsV}_6\text{O}_{13.2}$  in an asymmetrical lithium coin cell at different values of  $x$  for the high current pulse and PITT electrochemical methods. (A)  $\text{Li}_x\text{V}_2\text{O}_5$  cathode and (B)  $\text{Li}_x\text{V}_6\text{O}_{13.2}$  cathode.

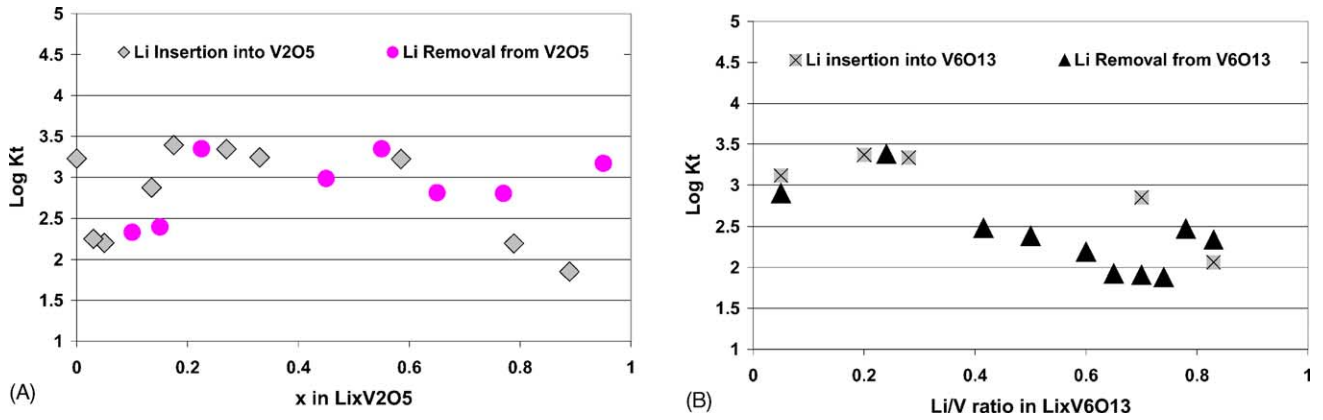


Fig. 6. The thermodynamic coefficients ( $K_t$ ) values for cathodes of  $\text{Li}/\text{Li}_x\text{V}_2\text{O}_5$  and  $\text{V}_6\text{O}_{13.2}$  at different values for  $x$  in an asymmetrical coin cell, calculated from kinetic data resulting from the application of the long-time potential step method. (A)  $\text{Li}_x\text{V}_2\text{O}_5$  cathode and (B)  $\text{Li}_x\text{V}_6\text{O}_{13.2}$  cathode.

method was thought by Honders et al. [5,6] typically to give only a rough indication of  $D$  but agreement with the other methods used in this study was very good. However, because of the large variation in charge passed, the change in the value of  $x$  was much larger than for the other methods, so the value of  $D$  obtained is only the average over a significant range of  $x$  in  $\text{Li}_x\text{V}_2\text{O}_{5-y}$ .

As can be seen in Fig. 5A and B for the calculation of chemical diffusion coefficients of  $\text{Li}^+$  ions in  $\text{Li}/\text{Li}_x\text{V}_2\text{O}_5$  and  $\text{nsV}_6\text{O}_{13}$  by different electrochemical methods, the agreement across the whole range of  $x$  is quite good. This good agreement comes despite having to estimate the thickness and the active electrode area in either method and the unique morphology of the cathode materials used. Such estimates have always been difficult to make for composite electrodes studied in the past. Although the cathode active material was crystalline, the surface was very rough, an initial assumption that the behaviour would be similar to the composite electrodes typically used for these measurements was born out by the results. The agreement with the diffusion coefficients for the Li ion insertion into  $\text{Li}_x\text{V}_2\text{O}_5$  was about  $10^{-8} \text{ cm}^2 \text{ s}^{-1}$  over the range of  $x = 0.1$  to 1.0, in agreement with the value reported by other groups [11,12] (see Fig. 5A). The thermodynamic coefficients ( $K_T$ ) for  $\text{Li}^+$  insertion into  $\text{Li}_x\text{V}_2\text{O}_5$  and  $\text{Li}_x\text{V}_6\text{O}_{13}$  was fairly consistent from  $x = 0.1$  to 0.9, with little difference between the two oxides (Fig. 6). No changes greater than about one order of magnitude, indicates that the layered structure of these oxides does not break down during cycling for this range of  $x$ .

## 5. Conclusions

Results have shown that the electrochemical properties of vanadium oxide bronzes made by an electrodeposition method could be examined. All the electrode active material was in electrical contact with the stainless steel mesh substrate and well-exposed to the electrolyte. These cathodes adhere very well to the substrate, with no binders or electronic conductors necessary. The initial oxidation state of the vanadium ion in the bronze was not found

to significantly influence the transport properties of the bronzes and the results agreed very well with those reported in the literature. These bronze cathodes have similar transport properties to composite cathodes, making them potentially useful for electrochromic displays and microbatteries.

The different techniques used to calculate the transport properties displayed good agreement across the range of  $x$  used. The use of the high current pulse technique could provide good transport data for an asymmetrical cell in a very short time compared with other methods. It is still limited, however, by the fact that electrolyte decomposition can occur at high voltages, but when used in tandem with other methods, can be quite effective in determining the transport properties of lithium coin cells.

## Acknowledgements

The authors wish to thank Giulio Torlone of the National Research Council, Institute for Chemical Process and Environmental Technology for technical assistance.

## References

- [1] B.W. Faughnan, R.S. Crandall, M.A. Lampert, *Appl. Phys. Lett.* 27 (1975) 275.
- [2] B.W. Faughnan, R.S. Crandall, *Topics in applied physics, Display Devices* 40 (1980) 180.
- [3] E. Andrukaitis, P.W.M. Jacobs, J.W. Lorimer, *Solid State Ionics* 37 (1990) 157.
- [4] E. Andrukaitis, G.L. Torlone, I.R. Hill, *J. Power Sources* 81–82 (1999) 651.
- [5] A. Honders, J.M. der Kinderen, A.H. van Heeren, J.H.W. deWitt, G.H.J. Broers, *Solid State Ionics* 15 (1985) 265.
- [6] A. Honders, G.H.J. Broers, *Solid State Ionics* 15 (1985) 173.
- [7] M.D. Levi, E.A. Levi, D. Aurbach, *J. Electroanal. Chem.* 421 (1997) 9–17.
- [8] E. Andrukaitis, *J. Power Sources* 54 (1995) 470.
- [9] E. Andrukaitis, *J. Power Sources* 119–121 (2003) 205.
- [10] K.M. Abraham, *J. Power Sources* 7 (1981–1982) 1.
- [11] N. Kumagai, I. Ishiyama, K. Tanno, *J. Power Sources* 20 (1987) 193.
- [12] P.G. Dickens, G.J. Reynolds, *Solid State Ionics* 5 (1981) 331.